

## STRUCTURAL, OPTICAL AND ELECTRICAL PROPERTIES OF ANNEALED Sb-DOPED CuInS<sub>2</sub> THIN FILMS GROWN BY THERMAL EVAPORATION METHOD

M. BEN RABEH\*, N. CHAGLABOU, M. KANZARI

*Laboratoire de Photovoltaïque et Matériaux Semi-conducteurs -ENIT BP 37, Le belvédère 1002-Tunis, Tunisie*

Structural optical and electrical properties of undoped and Sb-doped CuInS<sub>2</sub> thin films grown by single source thermal evaporation method on coming 7059 glass substrates heated at 100°C were studied. Sb species was mixed in the starting powders. The amount of the Sb source was determined to be in the range 0-4 Wt % molecular weight compared with the CuInS<sub>2</sub> alloy source. The films were annealed in vacuum at temperature of 200°C and in air atmosphere at temperature of 400°C for 2h. The effect of these annealing atmospheres on the properties of the films was studied by means of X-ray diffraction (XRD), optical reflection and transmission and resistance measurement. All the CuInS<sub>2</sub>/Sb films have relatively high absorption coefficient between  $2.10^4\text{cm}^{-1}$  and  $10^5\text{cm}^{-1}$  in the visible and the near-IR spectral range. We found that Sb-doped CuInS<sub>2</sub> thin films exhibit p-type conductivity and air annealing exhibit n-type conductivity.

(Received February 25, 2009; accepted February 28, 2009)

*Keywords:* Thin films; CuInS<sub>2</sub>; doping; Solar cells.

### 1. Introduction

Ternary chalcopyrite CuInS<sub>2</sub> thin films exhibit many excellent physical and chemical properties such as high absorption coefficient of almost  $10^5\text{cm}^{-1}$  in the visible spectral range [1], high tolerance to the presence of defects [2], an direct band gap closes to 1.5 eV, the optimum value for the photovoltaic conversion of solar energy [3], possibility to avoid n and p-type conductivity [4] and high chemical stability. In contrast to other ternary semiconductor materials, CuInS<sub>2</sub> is nontoxic, low-cost and easy to fabricate by various thin film deposition techniques [5-7]. For controlling a conduction type and obtaining low resistivity, several impurities doped CuInS<sub>2</sub> bulks have been studied. In several studies, it was shown that the structural, optical and electrical properties of CuInS<sub>2</sub> thin films could be obviously improved by optimized deposition conditions and doping [8-10]. Additionally, the electrical properties of CuInS<sub>2</sub> thin films could be modified by thermal in a reducing atmosphere [11,12]. Akaki et al [13] studied the structural, electrical and optical properties of Bi-CuInS<sub>2</sub> thin films grown by vacuum evaporation method. Zribi et al [8] investigated the effect of Na doping on the properties of CuInS<sub>2</sub> thin films and obtained more interesting results. The incorporation of iron during the crystal growth of CuInS<sub>2</sub> by chemical vapor transport was studied [14,15] and the results of electrical and photoluminescence measurements of P-doped and Zn-doped CuInS<sub>2</sub> crystals were reported [16]. T. Yamamoto et al [9] investigated the electronic structures of n-type doped CuInS<sub>2</sub> crystals using Zn and Cd species and showed that p-type doping using the group V elements such as N, P and As increases the Madelung energy, which gives rise to instability of ionic charge distribution in p-type doped CuInS<sub>2</sub> crystals [17]. Enzenhofer et al [10] showed that the open circuit voltage of solar cells based on CuInS<sub>2</sub> can be enhanced via controlled doping of small amounts of Zinc. In our previous paper [18] the incorporation of the doping element Sn in CuInS<sub>2</sub> was succeeded by annealing the Sn-doped films in vacuum. In this paper, we report on structural, optical and electrical properties of the Sb-doped CuInS<sub>2</sub> thin films after annealing in vacuum and in air atmosphere.

## 2. Experimental

### 2.1. Synthesis of targets and films

Amount of the elements of 99.999% purity Cu, In, S and Sb, five different powders of  $\text{CuInS}_2/\text{Sb}$  (0,1,2,3 and 4 Wt % molecular weight) were prepared. X-rays diffraction of powders analysis showed that in all cases the principal phase present in the ingots is the  $\text{CuInS}_2$ . Crushed powder of every ingot was used as raw material for the thermal evaporation. The Sb-doped  $\text{CuInS}_2$  thin films were deposited on corning 7059 glass substrates heated at 100 °C by single source thermal evaporation method in vacuum at  $10^{-6}$  torr. After what the films were annealed in vacuum at temperature of 200°C and in air atmosphere at temperature of 400°C for 2 h.

### 2.2. Characterization techniques

The structure of the  $\text{CuInS}_2/\text{Sb}$  samples was investigated using D8 Advance diffractometer. The optical characteristics were determined at normal incidence in the wavelength range 300 to 1800 nm using a Shimadzu UV/Vis-spectrophotometer. The resistance was measured using a digital universal meter and the type of conductivity of these films was determined by the hot probe method. Film thicknesses were measured by interference fringes method [19] and were in the range of 450-750 nm.

## 3. Results and discussion

### 3.1. Structure of targets and films

**Figure 1** shows the X-ray diffraction patterns of undoped and Sb-doped  $\text{CuInS}_2$  thin films after annealing in vacuum at 200°C. It can be seen that samples presented a sharp peak at  $2\theta = 27.9^\circ$  assigned to the (112) reflection of  $\text{CuInS}_2$  phase for the samples doped 0, 1,2 and 3 % Sb molecular weight and become highly oriented when the Sb content is 4 % molecular weight. We note also some additional diffraction peaks at  $26.49^\circ$  and  $43.4^\circ$ , which can be associated to binary compounds  $\text{In}_6\text{S}_7$  and Cu crystal. **Figure 2** shows the X-ray diffraction patterns of the films after annealing in air atmosphere at temperature of 400°C for 2 h. All the annealed films are oriented (112) plane and there is an improvement in the growth of the films after annealing in air for all the samples containing antimony. On the other hand, few minor peaks with lower intensities, associated to copper Cu,  $\text{CuO}$  and  $\text{In}_6\text{S}_7$  phases, can be observed from the patterns.

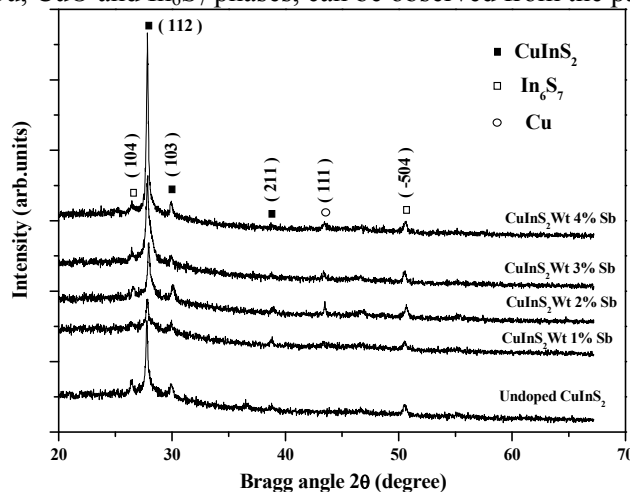


Fig. 1 X-ray diffraction patterns after annealing in vacuum.

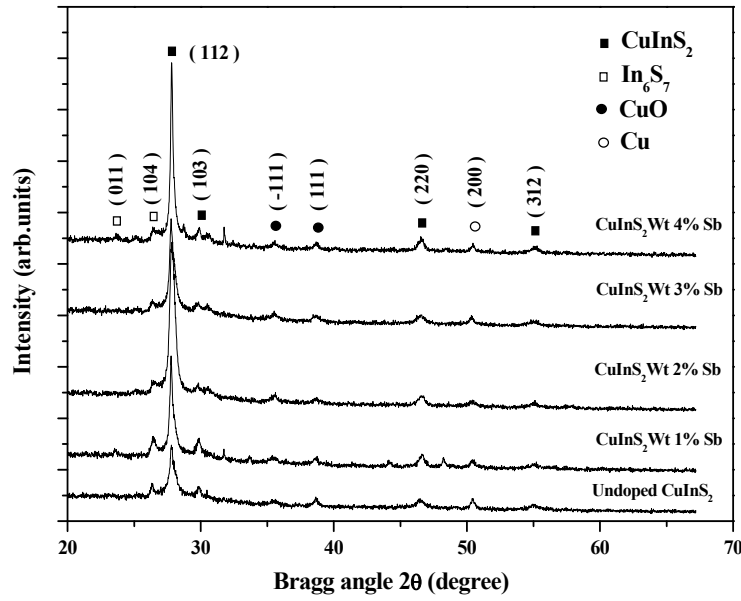


Fig.2. X-ray diffraction patterns after annealing in air atmosphere.

In the other hand the grain size along the (112) peak can be evaluated by using the Debye Scherer relation:

$$L = \frac{0.9\lambda}{\cos \theta_0 \Delta(2\theta)} \quad (1)$$

Where  $\lambda$  is the wavelength of the X-ray radiation used,  $\Delta(2\theta)$  the half intensity width of the peak and  $\theta_0$  the Bragg angle. The grain sizes are in the range 20 – 50 nm for all the samples undoped and Sb-doped.

### 3.2. Optical properties

To calculate the absorption coefficient  $\alpha(h\nu)$ , the following relation was used [20].

$$\alpha = \frac{1}{d} \ln \left[ \frac{(1-R)^2}{T} \right] \quad (2)$$

Where  $d$  is the film thickness, R and T are the reflection and transmission coefficient, respectively. **Figure 3** shows the dependence of the absorption coefficients  $\alpha$  versus the photon energy  $h\nu$  of the Sb-doped CuInS<sub>2</sub> thin films after annealing in vacuum. The films have relatively high absorption coefficients between  $2 \cdot 10^4 \text{ cm}^{-1}$  and  $10^5 \text{ cm}^{-1}$  in the visible.

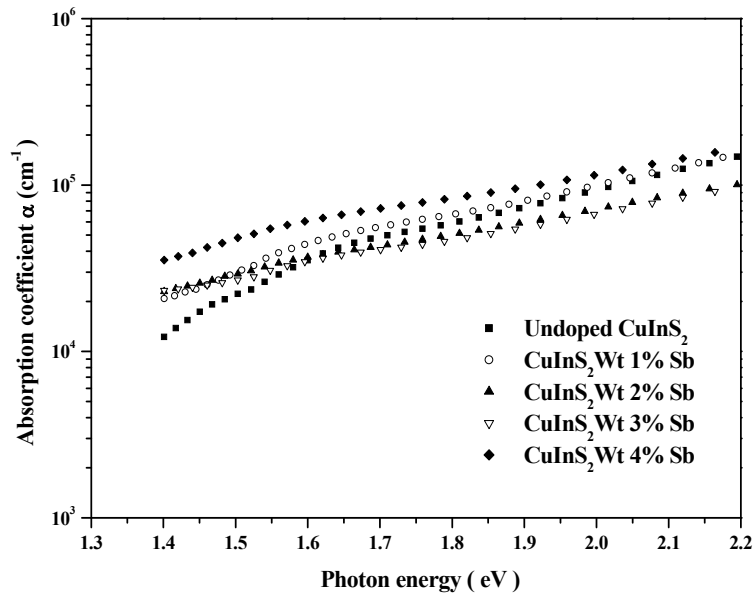


Fig. 3 Absorption coefficients spectra after annealing in air vacuum.

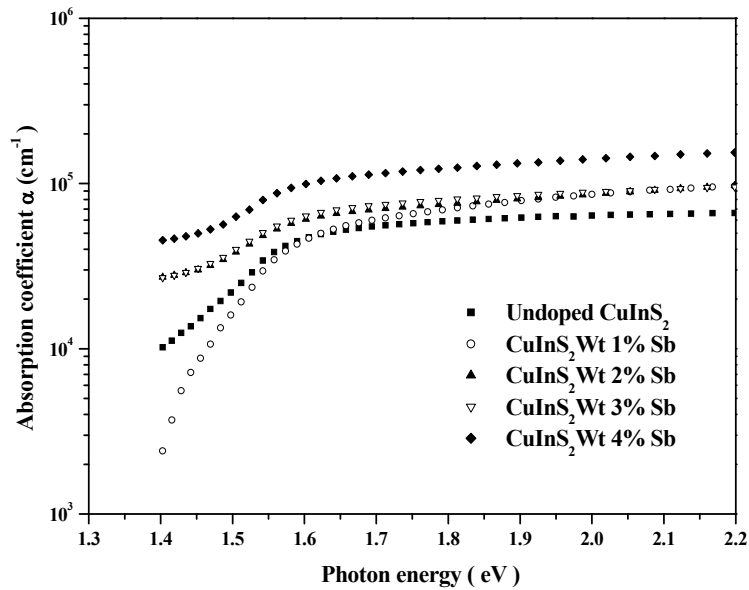


Fig. 4 Absorption coefficients spectra after annealing in air atmosphere.

Fig. 4 shows the absorption coefficients versus the photon energy for the Sb-doped  $\text{CuInS}_2$  thin films after annealing in air atmosphere. It is clear that the absorption coefficient increases with increasing Antimony % molecular weight. All the films have relatively high absorption coefficients more than  $5 \cdot 10^4 \text{ cm}^{-1}$  and remain constant along visible spectral range, which reached  $10^5 \text{ cm}^{-1}$  for the  $\text{CuInS}_2$  samples doped 4 Wt % Sb molecular weight. In the other hand, the relation between the absorption coefficients  $\alpha$  and the incident photon energy ( $h\nu$ ) can be written for direct allowed band gap as:

$$(\alpha h\nu)^2 = A(h\nu - E_g) \quad (3)$$

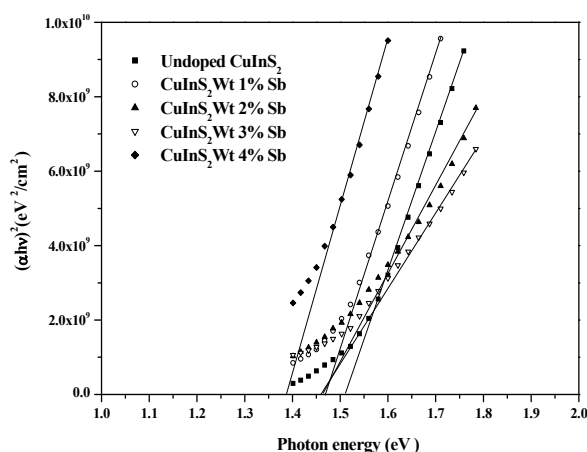


Fig. 5 Relationship between  $(\alpha hv)^2$  and photon energy after annealing in vacuum.

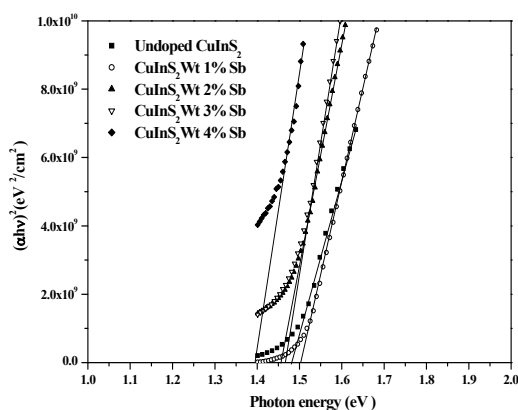


Fig. 6 Relationship between  $(\alpha hv)^2$  and photon energy after annealing in vacuum.

Where 'A' is constant and  $E_g$  is the optical band gap. To determine optical transition,  $(\alpha hv)^2$  versus  $hv$  was plotted, and the corresponding band gaps were obtained from extrapolating the straight portion of the graph on the  $hv$  axis at  $(\alpha hv)^2 = 0$  (Figures 5 and 6). It is now well established that  $\text{CuInS}_2$  is a direct gap semiconductor [21], with the band extrema located at the centre of the Brillouin. The direct band gap energy (Figure 7) decreases from 1.51 to 1.39 eV with increasing Sb content (0 to 4% molecular weight) for samples annealed in vacuum and in air atmosphere.

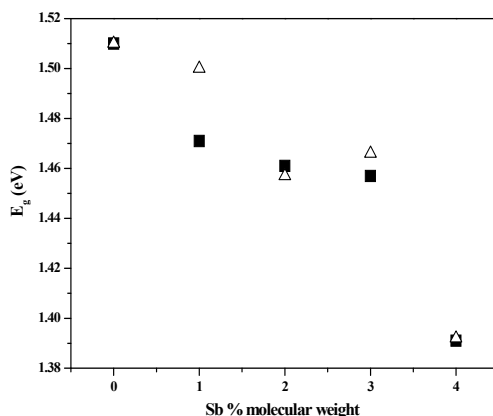


Fig. 7 Relationship between the optical bands gaps of  $\text{CuInS}_2/\text{Sb}$  with different Sb % molecular weight (Square) After annealing in vacuum and (Triangle) After annealing in air.

### 3.2. Electrical properties

Besides the optical properties, the electrical properties are also an important aspect of the performance of Sb-doped  $\text{CuInS}_2$  thin films. After annealing in vacuum (**figure 8.a**), all the films presented moderate lower electrical resistivity with p-type conductivity for the samples doped wt 4% Sb molecular weight. The resistivity decreases from  $5.51 \cdot 10^2 \text{ } \Omega\cdot\text{cm}$  to  $1.6 \cdot 10^2 \text{ } \Omega\cdot\text{cm}$  with increasing Sb content. After annealing in air atmosphere, the resistivity values decreases from 1.32 to  $0.22 \text{ } \Omega\cdot\text{cm}$  (**Figure 8.b**). All the undoped films and doped with 1,2,3 and 4 wt % Sb molecular weight exhibit high N-type conductivity. We note also an evolution from the P-type conductivity to the N-type conductivity for the  $\text{CuInS}_2$  sample doped with 4% Sb molecular weight. After annealing, all samples indicate low resistivity. One of the reasons is that probably the concentrations of donor and/or acceptor impurities in all  $\text{CuInS}_2$  samples may not change by Sb-doping. Indeed in our previous works [18] we show that the undoped  $\text{CuInS}_2$  films were converted to irreversible n-type conductivity after annealing in air atmosphere with low resistivity if the annealing temperature is higher  $200^\circ\text{C}$ . The XRD results indicate the same secondary phase (CuO) in both cases and no antimony oxide were detected. Perhaps the n-type Sb doped  $\text{CuInS}_2$  thin films are more stables than the n-type  $\text{CuInS}_2$ . However this proposition needs more studies to confirm it.

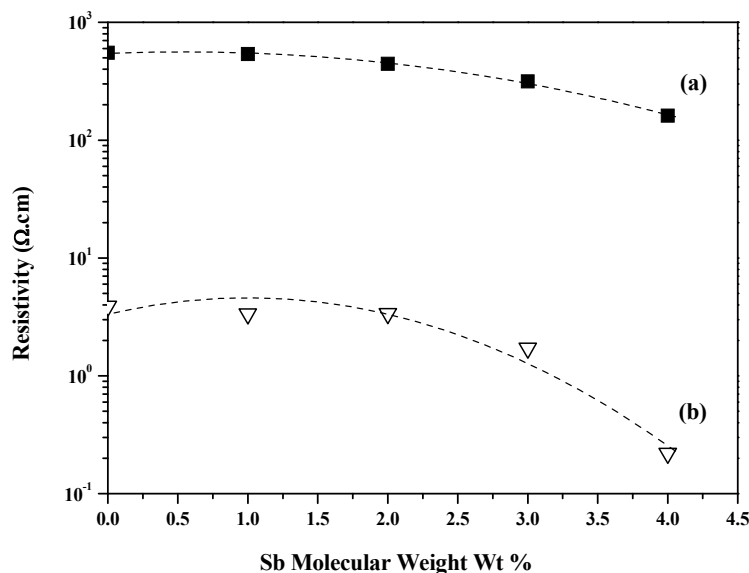


Fig. 8 Resistivity versus Sb % molecular weight of undoped and Sb-doped  $\text{CuInS}_2$  thin films (a) After annealing in vacuum and (b) After annealing in air atmosphere.

### 4. Conclusions

The effects of antimony incorporation on the structural, optical and electrical properties of  $\text{CuInS}_2$  thin films were studied. Sb species was mixed in the starting powders for different Sb % molecular weight. Undoped and Sb doped  $\text{CuInS}_2$  thin films grown by single source thermal evaporation method on Corning 7059 glass substrates heated at  $100^\circ\text{C}$  were deposited and subsequently annealed in vacuum at temperature of  $200^\circ\text{C}$  and in air atmosphere at temperature of  $400^\circ\text{C}$  for 2h. The absorption coefficients deduced from optical measurements are greater than  $2 \cdot 10^4 \text{ cm}^{-1}$  in the range 1.4-2.2 eV and remains constant along the visible spectral range with a value of  $10^5 \text{ cm}^{-1}$  for the  $\text{CuInS}_2$  doped wt 4% Sb molecular weight after annealing in air atmosphere. The Sb-doped samples after annealing have bandgap energy of 1.39-1.51 eV. The resistivity of the films decreases from  $5.51 \cdot 10^2$  to  $1.61 \cdot 10^2 \text{ } \Omega\cdot\text{cm}$  as the Sb % increases from 0 to 4

wt % molecular weight after annealing in vacuum and from 3.9 to 0.22  $\Omega$ .cm after annealing in air atmosphere. As-deposited CuInS<sub>2</sub> samples doped wt 4% Sb molecular weight are p-type conductivity and an evolution to high n-type conductivity for all the samples after annealing in air at critical temperature of 200°C for undoped samples and 100°C for doped ones.

## References

- [1] Siemer K., Klaer J., Luck I., Bruns J., Klenk R., Braunig D. Sol. Energy Mater. Sol. Cells., **67** (2001), 159.
- [2] Aksenov I., Sato K. J. Appl. Phys., **31** (1992), 2352.
- [3] Scheer R., Diesner K., Lewerenz H-J. Thin Solid Films., **168** (1995), 130.
- [4] Shay J.L., and Wernick J.H., Ternary Chalcopyrite Semiconductors, Growth, Electronic Properties and Applications ( Pergamon Press, New York, 1975).
- [5] Hashimoto T., Mercedes S., Takayama N., Nakayama H., Nakanishi H., Chichibou S.F., Ando S., in: W. Palz, H. Ossenbrink, P. Helm (Eds.), 20th European Photovoltaic Solar Energy Conference, Proceedings of the International Conference, Barcelona, June 6 – 10, 2005 p. 1926.
- [6] Zribi M., Kanzari M., Rezig B., in: W. Palz, H. Ossenbrink, P. Helm (Eds.), 20th European Phtovoltaic Solar Energy Conference, Proceedings of the Internatinal Conference, Barcelona, June 6– 10, 2005, p. 1890.
- [7] McNatt J.S., Dickman J.E., Hepp A.F., Kelly C.V., Jin M.H.C., Banger K.K., Conference Record of the 31st IEEE Photovoltaic Specialists Conference, Lake Buena vista, Florida, january 3 – 7, 2005, p. 375.
- [8] Zribi M., Kanzari M., Rezig B. Jpn J. Appl. Phys., **29** (2005), 203.
- [9] Yamamoto T., Luck V., Scheer R. Applied Surface Science., **159 – 160** (2000), 350.
- [10] Enzenhofer T., Unold T., Scheer R., Schock H.W., Material Research Society, 2005 Spring Proceedings, San Francisco, CA Spring Meeting March 28-April 1 2005.
- [11] Abaab M., Kanzari M., Rezig B., Brunel M. Solar Energy Materials & Solar Cells., **59** (1999), 299.
- [12] Ben Rabeh M., Kanzari M., Rezig B. Thin Solid Films., **515** (2007), 5943.
- [13] Akaki Y., Matsuo H., Yoshino K. Phys Stat Sol (c)., **8** (2006), 2597.
- [14] Brandt G., Ranber A., Schneider J. Solid St.Comm., **12** (1983), 481.
- [15] Binsma J.J.M., Giling L.J., Bloem J., Lumirrex J. **27** (1982), 35.
- [16] Uengt H.Y., Hwang H.L. J. Phys. Chem. Solids., **51** (1990), 11.
- [17] Yamamoto T., Yoshida H.K. Jpn. J. Appl. Phys., **35** (1996), L1562.
- [18] Ben Rabeh M., Zribi M., Kanzari M., Rezig B. Materials Letters., **59** (2005), 3164.
- [19] Heavens O.S., *Optical Properties of thin Solid Films, Butterworths, London, 1950.*
- [20] Milovzorov D.E., Ali A.M., Inokuma T., Kurata Y., Suzuki T, Hasegawa S. Thin Solid Films., **382** (2001), 47.
- [21] Nishikawa N.N., Aksenov I., Sinzato T., Sakamoto T., Sato K. Japan.J.Appl.Phys., **34** (1995), L975.